INFLUENCE OF MANGANESE ON THE MICROSTRUCTURE OF SECONDARY ALLOYS Al-Si-Mg

[1]Robert WIESZAŁA, [2]Jarosław PIĄTKOWSKI, [1]Jarosław KOZUBA

[1]*Silesian University of Technology, Faculty of Transport, Gliwice, Poland, EU,*
Robert.wieszala@polsl.pl, Jaroslaw.Kozuba@polsl.pl

[2]*Silesian University of Technology, Faculty of Metallurgy and Materials Engineering, Gliwice, Poland, EU,*
Jaroslaw.Piatkowski@polsl.pl

https://doi.org/10.37904/metal.2019.769

Abstract

The paper determines the influence of presence of various manganese content (0.2; 0.4 and 0.6 wt%) on the course of the crystallisation process, mechanical properties and structure of alloy AlSi10Mg. Recycled secondary materials with elevated content of iron were used to prepare the cast of this silumin. It was found that about 0.6 wt% of Mn causes the disappearance of the adverse, brittle phase β-Al_5FeSi in favour of phase α-$Al_{15}(FeMn)_3Si_2$, which crystallises in the form of evenly distributed in the metallic matrix of solution α (Al) with concentrated precipitations sized approximately 7-8 μm. The change of the adverse morphology of brittle eutectics containing Fe causes a slight increase of mechanical properties without the decrease of plasticity of alloys Al-Si-Mg-Mn used mainly as gravity die casting or pressure die casting. Manganese is therefore a "morphological corrector" of phase β in favour of privileged precipitations of α-$Al_{15}(FeMn)_3Si_2$. Taking into account the economic aspects and ecological conditions it seems reasonable to apply manganese in order to increase the presence of secondary Al alloys rather than the primary elements.

Keywords: Silumin, mechanical properties, alloys Al-Si-Mg

1. INTRODUCTION

Casting alloys Al-Si-Mg are applied in many sectors of the industry due to their very good mechanical and casting properties. Small thermal expansion, good corrosion resistance and relative strength cause that those alloys are valuable materials in preparation of the gravity die casting or pressure die casting which are thin-walled and with complex geometry. Therefore, those alloys are popular construction material in production of various parts which are under the influence of big or changeable thermodynamic loads, i.e. in automotive industry or aviation industry [1-6].

Due to high prices of electricity, growing costs of environmental protection and decreasing amounts of resources of bauxites the dynamics of production of primary Al has significantly decreased [7,8]. Therefore, it is more and more important to meet the demand for Al alloys with the use of recycled materials which is at present a significant amount of overall consumption in Europe and in the world with a constantly upward trend [8-10].

In order to meet the requirements of chemical composition and to provide good deformability of structural castings the alloys need to possess normative content of inclusions and gas impurities. In casting Al alloys, the chemical element which significantly lowers the mechanical properties such as elongation or impact strength and impedes the machinability of castings, is mainly iron [11-15]. The factors which are responsible for excessive brittleness of Al alloys and their reduced susceptibility to plastic processing are mainly precipitations of brittle intermetallic phases β-Al_5FeSi and $_{\alpha H}$-Al_8Fe_2Si which are similar in shape to "Chinese handwriting" [16-18]. Such phases in casting condition crystallise in the form of plates of needles with sharp edges and corners and cause propagation of micro-crackings and concentration of tension. Moreover, in alloys Al-Si-Mg there is a probability of formation of phase β-Al_9Fe_2Si with prismatic structure and ternary meta-stable

phases β-Al_4FeSi (25.4%Fe and 25.5%Si) and β-Al_3FeSi (33.9% Fe and 16.9% Si), which coagulate in case of lack of thermodynamic equilibrium [19, 20]. In those alloys with addition of metals (Mo, Cr, W and V) with content up to about 0.01 wt% an intermetallic phase $_{\alpha H}$-Al_8Fe_2Si can form with hexagonal structure and in case of higher content of the mentioned elements a phase $_{\alpha H}$-Al_8Fe_2Si with general stoichiometric formula $Al_X(FeMn)_YSi_Z$ can crystallise, where: x = 12; 15; 19, y = 3; 5, z = 1; 2; 3 [21-23].

The literature describes various methods of preventing crystallisation of harmful phase type β, which can be achieved by influencing the coagulation process of alloys Al-Si-Mg [24-26] or by adding Cr and Co which are phase elements of Al_7Cr; $Al_{13}CrFe_4Si_4$ and Al_9Co_2 [27-29].

Some papers [30-33] show that manganese is the chemical element which neutralises the negative influence of Fe in alloys of Al type. It was found that from 0.1 to 0.4 wt% of Mn dissolves in the solid solution of α(Al) which causes its strengthening and increase of fatigue strength, whereas the highest content of Mn (0.5-0.6 wt%) is mainly aimed at decreasing the negative influence of Fe on the machinability of the castings [23,30,32,34]. The authors of those papers suggest that manganese combines with Fe and forms AlFeMnSi compounds which crystallise in the form of precipitations with complex shapes. For example, the intermetallic phases $Al_{15}(FeMn)_3Si_2$ and $Al_{12}(FeMn)_3Si_2$ and multi-component eutectic α+Al(FeMn)Si which includes intermetallic phase $Al_{19}Fe_4MnSi_2$ considered as isomorphic with phase $Al_{20}Fe_5Si_2$.It is assumed that in those phases the manganese atoms take the positions of Fe atoms [23,32,35].

The aim of this paper was to test the influence of various content of manganese on the crystallisation process, structure and mechanical properties of secondary silumins $AlSi_{10}Mg$ with elevated content of Fe and to compare them with alloy achieved from primary elements. The aim therefore assumed the determination of characteristic crystallisation temperatures of phase elements and identification of main intermetallic phases which are present in tested alloys.

In order to complete the aims of the paper the range of tests included inter alia:

- analysis of crystallisation process of alloys with the use of Thermal Derivative Analysis (TDA - Polish abbreviation ATD),
- assessment of mechanical properties (*HB*, *Rm*, *Rp*, *A*),
- influence of Mn on the type and morphology of intermetallic phases of tested alloys.

2. MATERIAL AND METHODOLOGY OF TESTS

In order to test the influence of manganese addition on the mechanical properties there was an alloy AlSi10Mg (alloy No. 1) chosen and 0.2 wt% of Mn was added to it (alloy No.2), next one (alloy No.3) had 0.4 wt% Mn added and (alloy No.4) had 0.6 wt% added. Alloy No. 1 was prepared from primary materials which were: aluminium type 3N8 (99.98 % Al), silicon metal type 2202 (maximum wt% of impurities) and magnesium in the form of key metal with high purity. Alloys 2-4 were smelted from secondary elements and secondary foundry alloys. The alloy $AlMn_{30}$ was used as manganese carrier. A foundry alloy $AlSi_{13}Sr_9$ in the form of rods was used for modification. Every time the content of Sr in the alloy equalled 0.01-0.02 wt%.

The choice of alloy was justified with the wide application in industry, especially in transport, for example for pressure castings and gravity castings of elements of engines and structural elements of panelling of motor-car bodies.

Alloys were smelted in induction vacuum furnace VSG 02 Balzers in melting pot with capacity of 0.25 litre in argon atmosphere. Casting temperature equalled 740-750 °C. One part of the casting was casted to tester ATD-QC 4080 Heraeus Elektro-Nite (cooling temperature 30 °C·min^{-1}), Sand the second part to casting die made of copper in room temperature. Achieved castings served as material for chemical composition analysis, tests of mechanical and structural properties. The TDA (thermal derivative analysis - ATD) was conducted with temperature recorder Crystaldigraph NT3-8K, which meets the requirements of norms EN61010 and EN60584

in terms of industrial measurements with shell-form thermocouples NiCr-NiAl (type K). Program Analdta was used to visualise the crystallisation curves. After casting there was heat treatment applied to reach the condition of T6.

Static tension test was conducted in room temperature in accordance with norm EN ISO 6892-1 on device Instron 3382, with the use of ratio 20:1 and constant tension speed of 5 mm·min-1. There was resistance to tension (Rm) determined in test together with conventional yield point (*Rp*) and percentage of elongation after failure of test piece (A). Hardness measurement with the use of Brinell method was conducted on Zwick ZHF1device with load strength of 250 N using steel sphere with diameter of 5 mm in time of 35 s. There were 10 measurements made with exclusion of 2 extreme ones, and out of the remaining there was arithmetic mean calculated.

Metallographic tests were conducted on light microscope MeF-2 Reichert. X-ray microanalysis was conducted on scanning microscope Hitachi S-4200 coupled with x-ray spectrometer EDS Voyager, equipped with detector of secondary electrons SE and backscattered electrons BSE.

Analysis of chemical composition and surface distribution of chemical elements was conducted with the use of s-ray microanalysis with energy dispersion EDS on detector Thermo Noran. X-ray tests were conducted with the use of diffractometer X`Pert Philips, with the use of lamp λCuKα - 0.154178 nm, powered with current of 30 mA by 40 kV. Registration was performed with the use of step-scanning method every 0.04° and time of counting of 10 seconds in the angle range 2θ from 20° to 140°. There were Soller slits applied of 0.04 mm.

3. RESULTS OF TESTS

Results of chemical composition analysis of tested alloys are presented in **Table 1**.

Table 1 Results of chemical composition analysis of tested alloys[1] (Al - remainder) [own study]

No. of alloy	Name of alloy	Content of elements (wt%)							
		Si	**Fe**	**Mg**	**Mn**	**Cu**	**Ti**	**Sr**	other[2]
1	AlSi10Mg	10.22	0.13	0.91	-	0.02	0.03	0.011	0.05
2	AlSi10Mg+0.2%Mn	9.92	0.57	0.89	0.19	0.01	0.04	0.017	0.03
3	AlSi10Mg+0.2%Mn	10.17	0.59	0.98	0.38	0.01	0.03	0.011	0.04
4	AlSi10Mg+0.2%Mn	10.11	0.50	0.95	0.59	0.01	0.03	0.014	0.04

where: [1]results are arithmetic mean of 10 measurements, [2]sum of the remaining elements and impurities

Thermal derivative analysis was conducted in order to test the influence of various amounts of Mn on the course of crystallisation of tested alloys. With application of standard coefficients of smoothing for temperature curve in time (TA) and its first derivative (ATD) there were the following temperatures marked: $T_{liq.}$; $T_{E\min.}$; T_E; $T_{E(Mg)}$; $T_{E(Mn)}$ and T_{sol}. Diagram of ATD for alloy $AlSi_{10}Mg$ without Mn addition is shown in **Figure 1**. Due to the fact it was stated that addition of Mn does not significantly influence the course of curved TA and ATD below temperature T_E, **Figure 2** shows only a fragment of ATD diagram for alloy $AlSi_{10}Mg$ with addition of 0.2; 0.4 and 0.6 wt% Mn.

As presented on the diagram of thermal analysis ATD the crystallisation of alloy AlSi10Mg without addition of Mn (**Figure 1**), starts in temperature $T_{liq.}$ (575 °C) represented by point A. In this temperature the nucleation begins together with growth of dendrites of solid solution α(Al), which lasts to the moment when it reaches temperature of about 564 °C (point C **Figure 1**). Next, the nucleation begins together with growth of double eutectics α(Al)+β(Si), preceded by overcooling which last until reaching a temperature of about 553 °C (point D). Probably from that time the crystallisation of eutectics including Fe and eutectics α(Al)+Mg_2Si+β begins

which lasts till reaching a temperature of about 526 °C (point E in **Figure 1**). In this temperature the crystallisation of triple eutectics α(Al)+Mg_2Si+β ends and at the same time the solidification of the whole alloy ends.

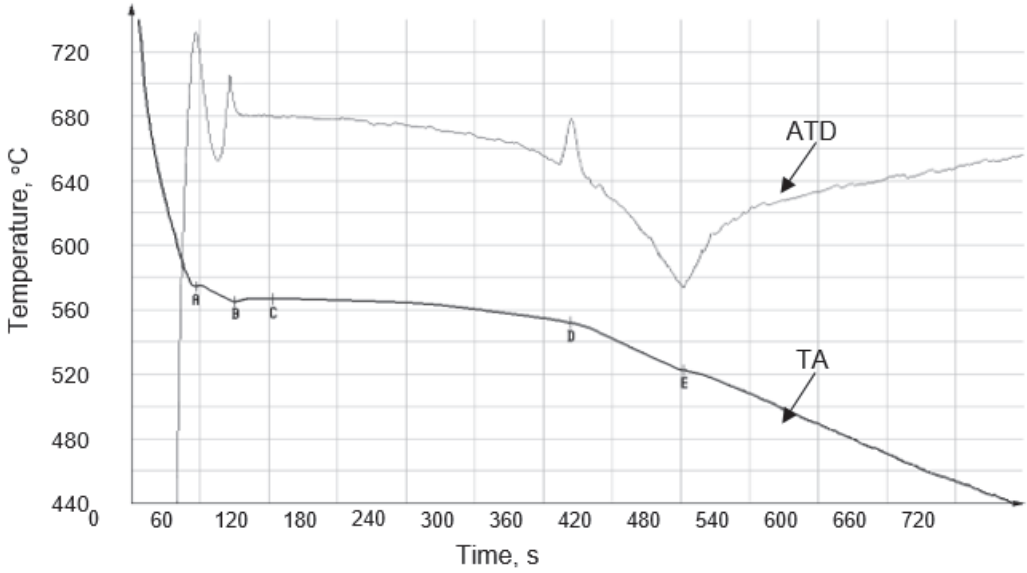

Figure 1 Diagram of ATD analysis (TDA) of alloy AlSi10Mg without addition of Mn with characteristic crystallisation points

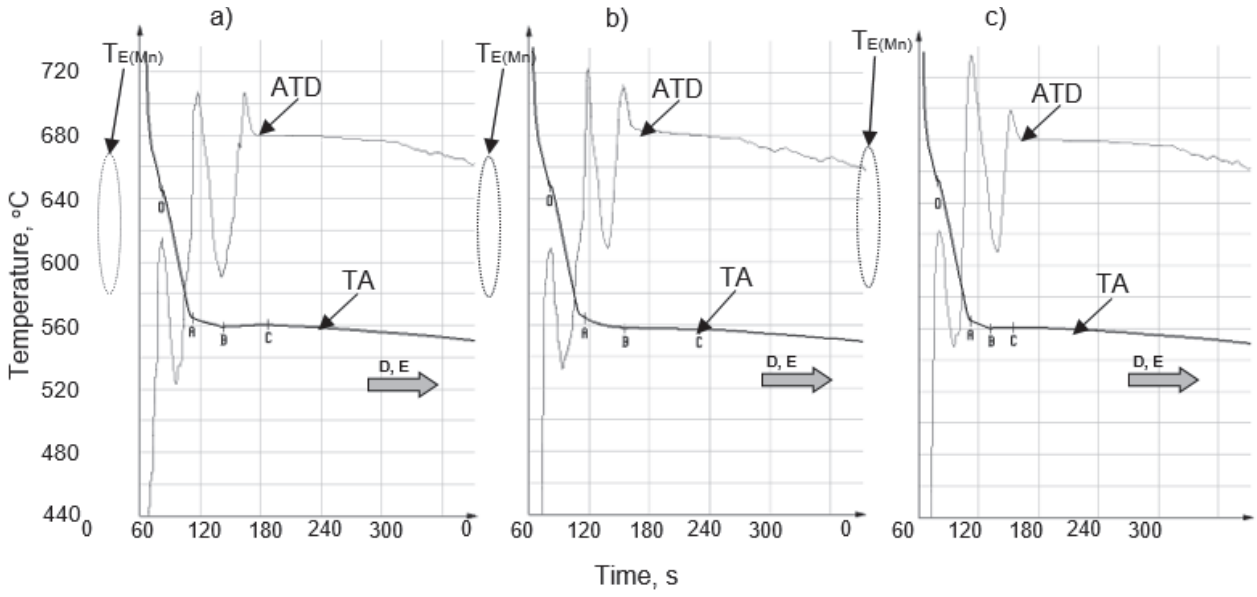

Figure 2 Fragment of ATD (TDA) diagram for alloy AlSi10Mg with characteristic crystallisation points: a) with addition of 0.2 wt% Mn; b) with 0.4 wt% Mn; c) with 0.6 wt% Mn

Presentation of characteristic values of crystallisation temperatures of tested alloys is shown in **Table 2**.

It results from the basis of analysis of ATD that besides the identification of characteristic temperature of microstructure elements crystallisation the method can also be applied to assess the quality of the casting materials. As it has already been mentioned, the purity of the alloy is assessed on the basis of the amount of impurities, mainly Fe content.

Table 2 Characteristic temperatures of crystallisation of tested alloys

No. of alloy	Name of alloy	Characteristic temperatures (°C) (points on diagrams TA and ATD)					
		0 $T_{E(Mn)}$	A $T_{liq.}$	B $T_{Emin.}$	C T_E	D $T_{E(Mg)}$	E $T_{sol.}$
1	AlSi10Mg	-	575	564	568	553	526
2	AlSi10Mg + 0.2 wt% Mn	646	572	558	563	549	520
3	AlSi10Mg + 0.4 wt% Mn	651	569	554	559	544	520
4	AlSi10Mg + 0.6 wt% Mn	657	569	555	560	543	521

where:

$T_{E(Mn)}$ - temperature of crystallisation of eutectic rich in manganese (°C)
$T_{liq.}$ - liquidus temperature (°C)
$T_{Emin.}$ - minimum temperature of crystallisation of binary eutectic α(Al)-β(Si) (°C)
T_E - temperature of crystallisation of binary eutectic α(Al)-β(Si) (°C)
$T_{E(Mg)}$ - temperature of crystallisation of eutectic rich in Fe (°C)
$T_{sol.}$ - solidus temperature (°C)

In alloys of Al type which are impure because of Fe content there are brittle phases: β-Al_5FeSi and $_{\alpha h}$-Al_8Fe_2Si (to 0.5 wt% Fe) and phase β-Al_9Fe_2Si which crystallise most often. Crystallisation of eutectics which include those phases should be visible on the curves TA and ATD. The possible exothermic effect can be expected after nucleation and dendrite growth of solid solution α(Al), that is in temperature range 575 °C-568 °C. However, as can be seen in **Figure 1** there are no heat effects resulting from nucleating and eutectics type α(Al)+Al_XFe_YSi+β(Si) growth. It is probably caused by such small thermal effect which comes from eutectics containing Fe that it is not noticeable on temperature curve. Therefore, tests should be supplemented with calorimetric measurements which were not the aim of this paper.

In case of crystallisation of alloy AlSi10Mg with addition of Mn (**Figure 2**) the course of curves TA and ATD in first phase of crystallisation is slightly different. Analysis of the phase equilibrium systems (double Al-Mn) and (triple Al-Si-Mn) [28] shows that as a result of peritectic reaction L+Al_4Mn↔α+Al_6Mn (in temperature of 708 °C) a phase Al_6Mn appears and in temperature of equilibrium 658 °C the double eutectic α+Al_6Mn nucleates. It can be also read from those systems that for alloys Al-Si-Mg with addition of Mn and Fe the intermetallic phases: β-Al_5FeSi, $_{\alpha C}$-$Al_{12}(FeMn)_3Si$ and $_{\alpha h}$-Al_8Fe_2Si can appear which are included in eutectic types $Al_X(FeMn)_YSi_Z$. In temperature range from 646 °C to 657 °C there is a significant exothermal effect observed (marked with point 0 in **Figure 2**). Taking this into account, it can be assumed that it is a beginning of nucleation and eutectics growth which includes the primary intermetallic phase rich in Mn. Temperature of its precipitation is therefore about 10 °C lower than equilibrium temperature of phase Al_6Mn crystallisation. Addition of manganese, independently from the amount, did not significantly influence the course of further crystallisation process of alloy $AlSi_{10}Mg$ and at the same time had no impact on the change of values of characteristic temperatures in tested alloys (points D and E in **Figure 2**).

4. RESULTS OF TESTS OF MECHANICAL PROPERTIES

Results of hardness measurements HB for tested alloys are shown in **Figure 3a**, and resistance to tension - **Figure 3b**, conventional yield point - **Figure 3c**, and elongation of sample on **Figure 3d**.

Analysis of results of mechanical properties (**Figure 3**) shows that in each case the heat treatment to the condition of T6 causes increase of tested properties in relation to condition of casting (without heat treatment).

This increase for alloy without manganese equals respectively: for *HB* 45 %, for *Rm* 44 %, for *Rp* 60 % and for elongation 30 %. Additionally, it should be mentioned that the addition from 0.2 to 0.6 wt% of Mn caused further elevation of tested properties which were the hardness increase of about 11 %, resistance to tension increase of about 20 % and conventional yield point increase of about 17 % in comparison with alloy without the addition of Mn. No significant change in elongation was observed after addition of manganese in range 0.2÷0.6 wt%. Increase of manganese content of over 0.6 wt% did not significantly influence on the elevation of mechanical properties of alloys Al-Si-Mg and therefore it can be assumed that the content of about 0.6 wt% of Mn is the optimum amount.

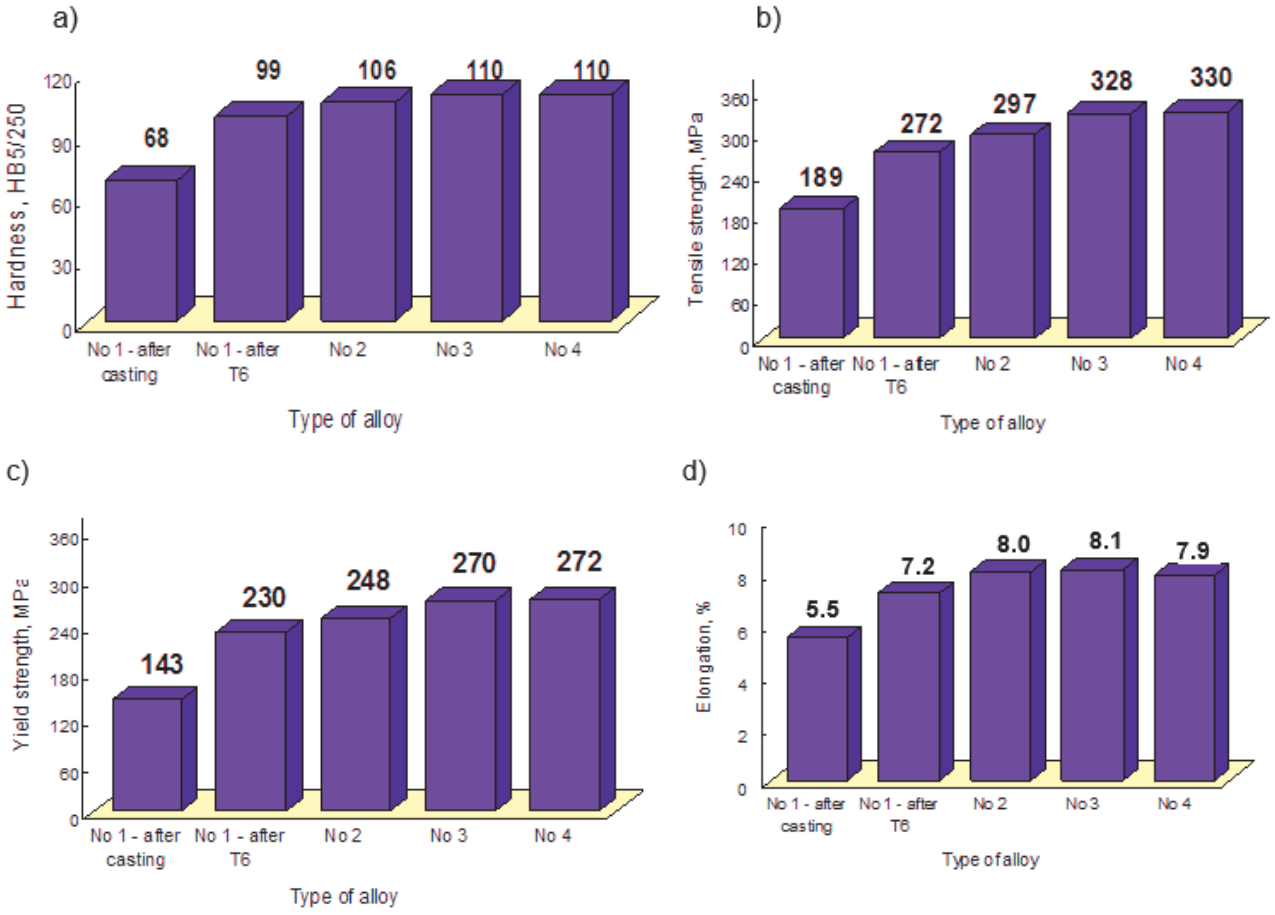

Figure 3 Results of measurements of mechanical properties of tested alloys: a) *HB*; b) *Rm*; c) *Rp*; d) elongation *A*

5. MICROSTRUCTURE TESTS RESULTS

Results of diffractometric tests of alloy $AlSi_{10}Mg$ without Mn and with addition of 0.6 wt% of Mn are presented in **Figure 4**. Analysis of microstructure tests, in particular the x-ray diffraction patterns (**Figure 4a**), has shown that in alloy $AlSi_{10}Mg$ without Mn, apart from the reflections coming from Al and Si there are also intermetallic phases:β-Mg_2Si and adverse phase β-Al_5FeSi. In alloys with addition of 0.2 and 0.4 wt% Mn there was phase β-Al_5FeSi found but its contribution has decreased. After adding 0.6 wt% Mn (**Figure 4b**) there was no phase β-Al_5FeSi present any more. However, there were intermetallic phases Al_9Fe_2Si and $Al_{15}(FeMn)_3Si_2$ identified. It can be read from ATD tests (**Figure 2**) that intermetallic phase α-$Al_{15}(FeMn)_3Si_2$ crystallised as primary and no contribution of manganese was found in content of other structure divisions and crystallising multi-component eutectics in tested alloys. Microstructure of alloy AlSi10Mg without addition of Mn in casting condition is presented in **Figure 5** and after addition of 0.6 wt% of Mn - in **Figure 6**.

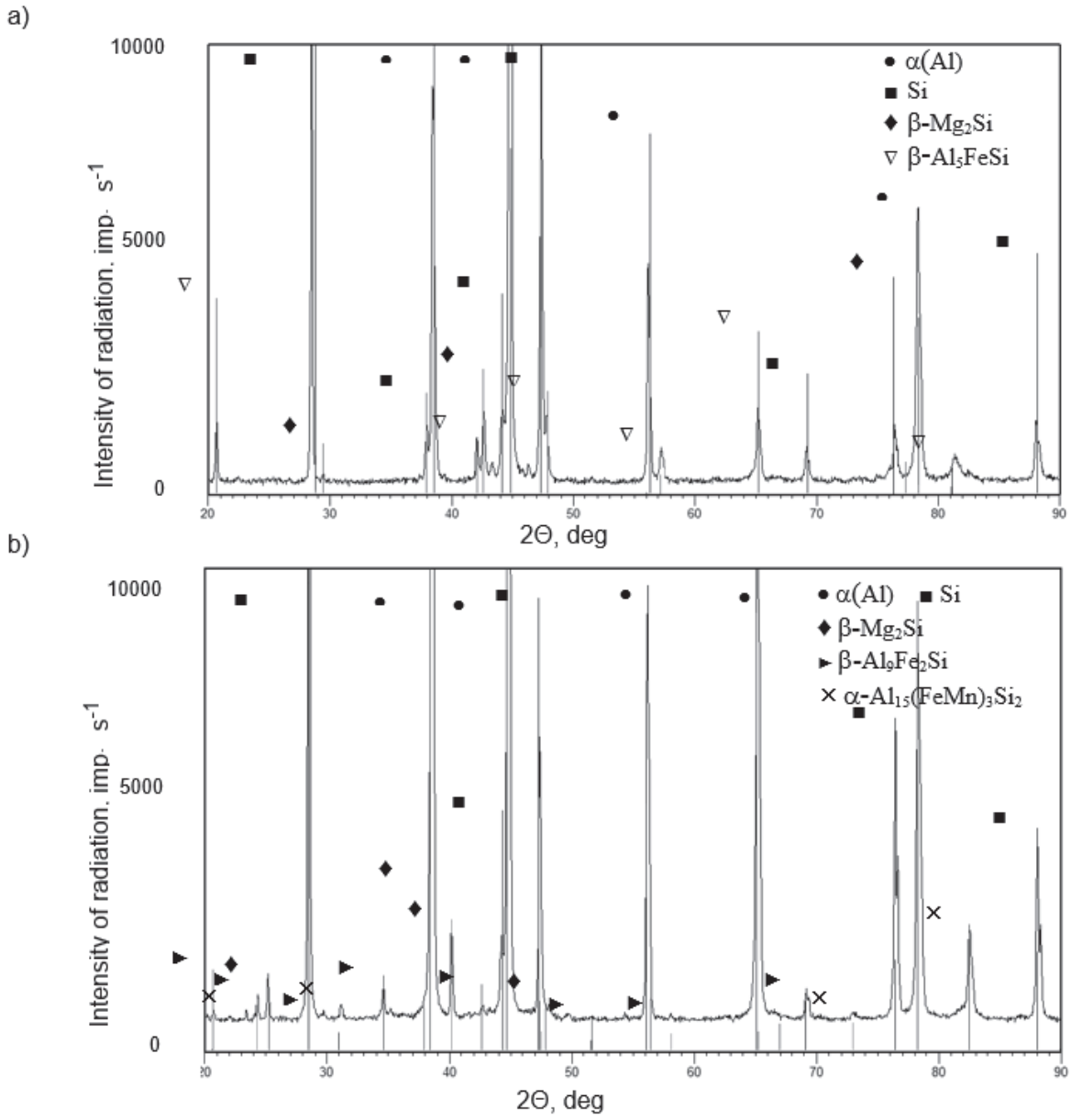

Figure 4 X-ray diffractometer of alloy AlSi10Mg: a) without Mn; b) with 0.6 wt% Mn

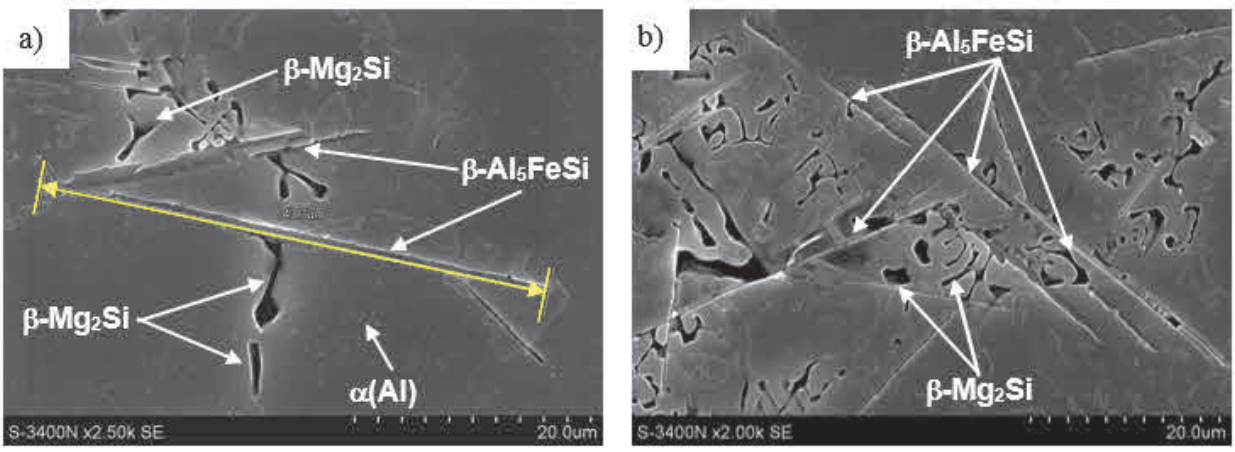

Figure 5 Microstructure of alloy AlSi10Mg without Mn (with different magnifications)

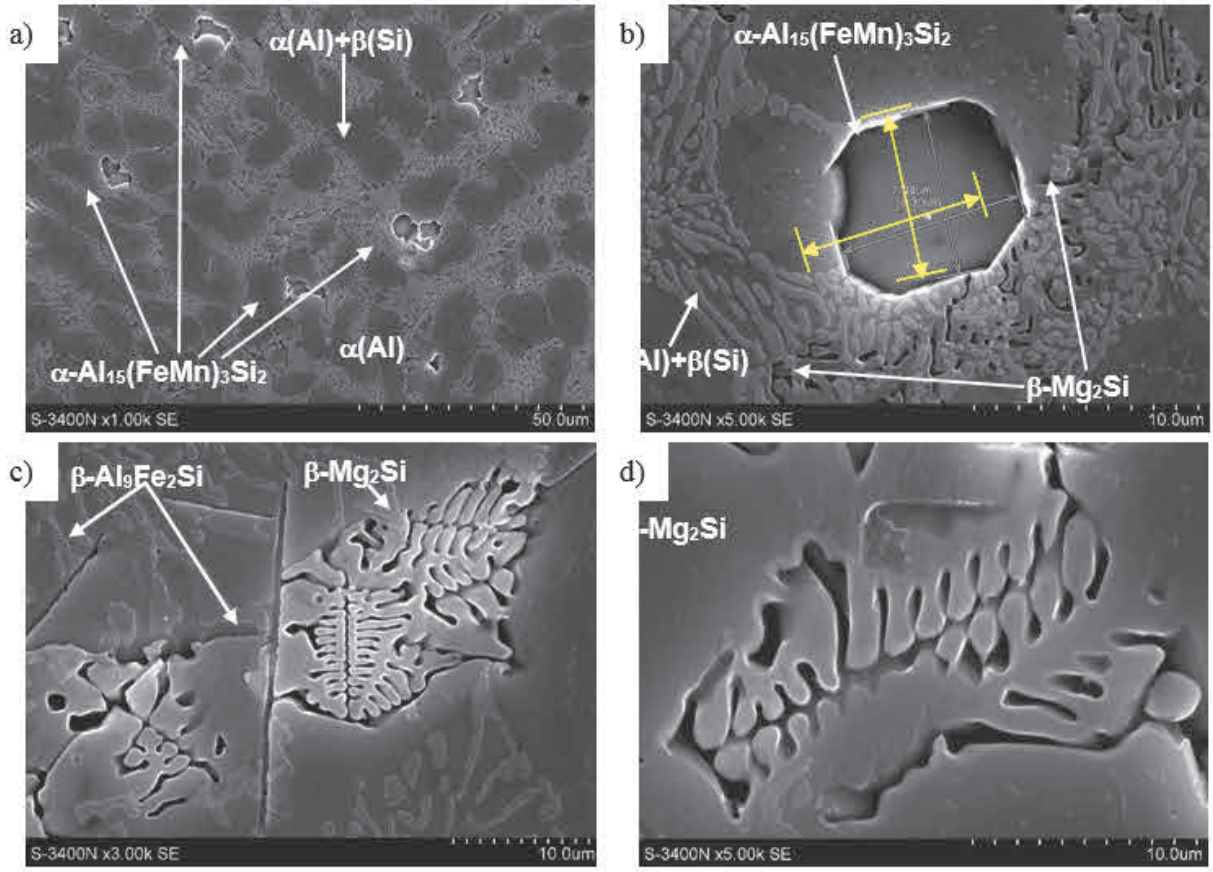

Figure 6 Microstructure of alloy $AlSi_{10}Mg$ with addition of 0.6 wt% Mn with characteristic phase divisions α-$Al_{15}(FeMn)_3Si_2$; β-Al_9Fe_2Si and β-Mg_2Si

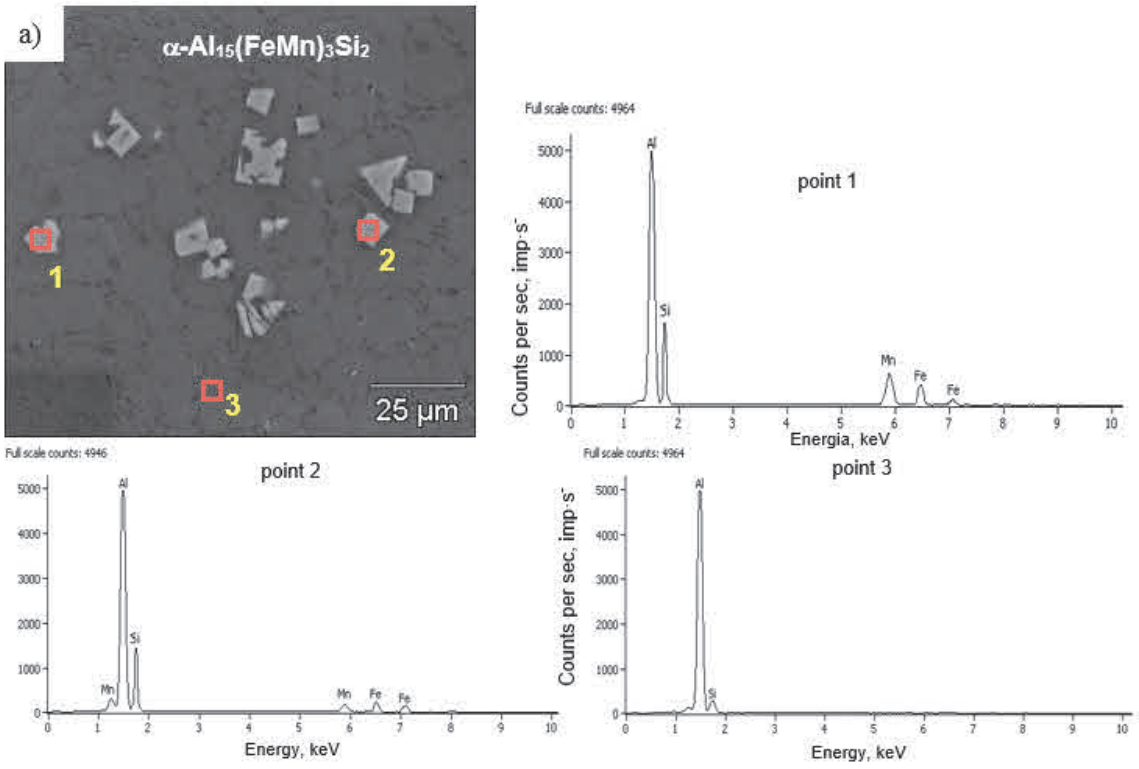

Measurement point	*Al-K*	*Si-K*	*Mn-K*	*Fe-K*	*Al-K*	*Si-K*	*Mn-K*	*Fe-K*
	(wt%)				(at%)			
pt1	75.1	12.9	8.8	3.2	75.3	12.4	8.5	3.8
pt2	75.9	12.1	9.0	3.0	74.8	12.2	9.1	3.9
pt3	98.7	1.3	-	-	98.5	1.5	-	-

Figure 7 Microstructure of alloy AlSi10Mg with addition of 0.6 wt% Mn and nuclear dispersed energy spectrum and chemical composition in points

Observations of microstructures show that in secondary alloys $AlSi_{10}Mg$ without manganese an adverse phase β-Al_5FeSi crystallises which reaches the length of up to 40 μm (**Figure 5a**) with needle-plate morphology. Divisions of this phase are disadvantageous because, as tests [16-18] show, they cause a concentration of local stress intensities and decrease of plasticity and susceptibility to cracking. In alloys with addition of Mn the phase β-Al_5FeSi does not form but phase β-Al_9Fe_2Si and α-$Al_{15}(FeMn)_3Si_2$ appear (**Figure 6b**). Phase β-Al9Fe2Si is also present in "needle" form but with smaller length (up to 20μm) - **Figure 6c**. It can be then assumed that the addition of manganese causes the disappearance of the disadvantageous phase β-Al_5FeSi in favour of α-$Al_{15}(FeMn)_3Si_2$ which crystallises in the form of compact, evenly distributed in the matrix of solid solution α(Al) polyhedral precipitations sized 7-8 μm - **Figure 6b**. In all tested alloys the intermetallic phase β-Mg_2Si crystallises in the characteristic shape which is similar to "Chinese handwriting" - **Figure 6d**. Microstructure of alloy $AlSi_{10}Mg$ with addition of 0.6 wt% Mn and nuclear dispersed energy spectrum and chemical composition in points is shown in **Figure 7**.

6. SUMMARY AND CONCLUSIONS

Growing prices of energy, decreasing amounts of natural raw materials and the necessity to protect the environment cause that the development of materials circulation is inevitable. In order to meet those demands and avoid dependence on primary aluminium import from outside Europe it is necessary to turn attention to recycling of secondary materials. It is also connected with non-ferrous metals, including Al alloys which are the main material for various types of castings in automotive and aviation industry branches.

Therefore, to meet the requirements of satisfactory plasticity and resistance comparable to the alloys prepared from primary raw materials it is necessary to maintain the impurities in secondary alloys on adequately low level. For casting alloys Al-Si the main impurity is Fe which has detrimental influence on the utility properties and was widely described in literature [11-15]. Therefore, it is justified to conduct research in order to decrease the detrimental influence of Fe on the mechanical and plastic properties of secondary Al alloys.

It was found, that among various additives which influence the change of shape and size of undesirable intermetallic phases type β manganese is the right "morphological corrector" of Al-Si alloys. In silumins which are not contaminated with Fe the most often crystallisation is phase β-Al_5FeSi with morphology in form of thin plates with sharp edges which can be seen in cross-section in forms of needles with length up to 40 μm. This phase decreases the mechanical properties and increases the susceptibility to cracking due to its brittleness. It was stated that manganese beneficially influences phase division β-Al_5FeSi and secondary alloys Al-Si-Mg with addition of manganese have satisfactory strength and plasticity. It is possible due to crystallisation of phase $Al_{15}(FeMn)_3Si_2$ which forms compact, polyhedral divisions sized 7-8 μm evenly distributed in solid solution matrix α(Al). It was also stated that the optimum content of manganese addition is about 0.6 wt% but there should be further tests conducted on the notion of the quotient of Mn to Fe. It is particularly important in case of slag formulation which impedes the achievement of high plasticity of pressure castings. Tests results on the optimum content of Mn to Fe in alloys Al-Mg-Si are presented in paper [36] whereas for alloys Al-Si-Cu

in paper [37]. Conclusions from these papers, however, cannot be directly applied in case of Al-Si-Mg alloys due to a totally different sequence of crystallisation and occurring intermetallic phases in those alloys.

Taking the above-mentioned statements into account, the following conclusions were formulated:

1) It can be read from the diagrams TA and ATD for alloys Al-Si-Mg-Mn that the intermetallic phase $Al_{15}(FeMn)_3Si_2$ undergoes primary nucleation and does not have big influence on the course of the remaining stages of crystallisation process.
2) Addition of 0.6 wt% of Mn causes replacement of adverse phase β-Al_5FeSi of "needle-plate" texture with primary intermetallic phase α-$Al_{15}(FeMn)_3Si_2$ which crystallises in the form of polyhedrons which are evenly distributed in the solution matrix α(Al). Unfortunately, it is hard to determine unambiguously the optimum quotient of Mn to Fe in alloys Al-Si.
3) Due to morphology and size of intermetallic phase α-$Al_{15}(FeMn)_3Si_2$ it may be assumed that it can positively influence the improvement of mechanical properties without a significant decrease of plasticity and the possibility of cracking of alloys Al-Si-Mg. It is the reason why castings prepared from secondary materials can serve as substitution of alloys prepared from primary raw materials.
4) It was also found, that in alloys Al-Si-Mg with addition of manganese a phase β-Al_9Fe_2Si crystallises in the "needle form", but with significantly smaller length (up to 20 μm).

REFERENCES

[1] ROBLES, Hernandes F.C., HERRERA, Ramirez J.M. and MACKAY R. *Al-Si Alloys. Automotive, Aeronautical, and Aerospace Application*. Springer International Publishing AG, 2017.

[2] ZAMANI, M. *Al-Si Cast Alloys - Microstructure and Mechanical Properties at Ambient and Elevated Temperature*. Inekao AB, Kållered, Sweden, 2015.

[3] MILLER, W. S. Recent Development in aluminum alloys for the automotive industry. *Materials Science and Engineering.* 2000. vol. A280, pp. 37-49.

[4] MACKENZIE, S.D. and Totten, G.E. *Analytical Characterization of Aluminum, Steel, and Superalloys.* Taylor and Francis Group. Boca Raton 2006.

[5] JAVIDANI, M. and LAROUCHE, D. Application of cast Al-Si alloys in internal combustion engine components. *International Materials Reviews.* 2014. vol. 59, no. 3, pp. 132-158.

[6] KAUFMAN, J.G., and ROOY, E.L. *Aluminum Alloy Casting - Properties, Processes, and Applications*. ASTM International, Materials Park, OH, USA, 2004.

[7] IDZIOR, M. Kierunki zmian materiałowych w motoryzacji w świetle wymogów ekologii. *MOTROL.* 2007. No. 9, pp. 72-87.

[8] STULGIS, G. Recykling aluminium - ogniwo gospodarki. *Recykling.* 2013. vol. 6, no. 150, pp. 22-24.

[9] SUBODH, Dr. and DAS K. Designing aluminum alloys for a recycling friendly word. *Materials Science Forum.* 2006. vol. 519-521, pp. 1239-1244.

[10] WILLIAM, T., CHOATE, J., and GREEN, A.S. *Modeling the Impact of Secondary Recovery (Recycling) on the U.S.,* Al Supply and Nominal Energy Requirements, TMS, 2004.

[11] DAWIS, J.R. *Aluminum and aluminum alloys.* ASM Specialty Handbook. 1998.

[12] CREPEAU, P. N. Effect of iron in Al-Si alloys: a critical review. *Transactions of the American Foundryman's Society.* 1995. vol. 103, pp. 361-366.

[13] DINNIS, C. M. As-cast morphology of iron-intermetallics in Al-Si foundry alloys. *Scripta Materialia.* 2005. vol. 53, no. 8, pp. 955-958.

[14] *Fatigue Data Book: Light Structural Alloys*. ASM International. The Materials Information Society. Materials Park, OH, USA 1995.

[15] *Aluminum Alloy Selection and Applications*. Published by the Aluminum Association. Inc New York. 1998.

[16] SAMUEL, A.M., SAMUEL, F.H. and DOTY, H.W. Observations on the formation of α-AlFeSi phase in 319 type Al-Si alloys. *Journal of Materials Science.* 1996. vol. 31, pp. 5529-5539.

[17] IRIZALP, S.G., and SAKLAKOGLU, N. Effect of Fe-rich intermetallics on the microstructure and mechanical properties of thixoformed A380 aluminum alloy. *Engineering Science and Technology an International Journal.* 2014, vol. 17, pp. 58-62.

[18] KHALIFA, W., SAMUEL, F.H., and GRUZLESKI, J.E. Iron intermetallic phases in the Al corner of Al-Si-Fe system. *Metallurgical and Materials Transactions.* 2003. vol. A34, no. 13, pp. 807-825.

[19] BELOV, N.A. and ESKIN, D.G. and AVXENTIEVA, N.N. Constituent phase diagrams of the Al-Cu-Fe-Mg-Ni-Si system and their application to the analysis of aluminum piston alloys. *Acta Materialia.* 2005. vol. 53, pp. 4709-4722.

[20] BELOV, N.A., AKSENOV, A.A. and ESKIN, D.G. *Iron in Aluminum Alloys.* Taylor & Francis, New York, 2002.

[21] KAMMER, C. *Aluminum Handbook: Fundamentals and Materials*. 1999. vol. 1, Oldenburg.

[22] KAMMAT, R.G., BUTLER, J.F., MURTHA, S.J. and BOVARD, S.F. Alloy 6022-T4E29 for automotive sheet application. *Materials Science Forum.* 2002. vol. 396, pp. 1591-1596.

[23] MRÓWKA-NOWOTNIK, G. *Rola składników fazowych w kształtowaniu mikrostruktury i właściwości mechanicznych stopów aluminium grupy 6xxx*. Oficyna Wydawnicza Politechniki Rzeszowskiej, Rzeszów, 2012.

[24] NARAYANAN, L.A., SAMUEL, F.H. and GRUZLESKI, J.E. Crystallization behavior of iron-containing intermetallic compounds in 319 aluminum alloy. *Metallurgical and Materials Transactions.* 1994. vol. 25A, pp. 1761-1773.

[25] FANG, X., SHAO, G., LIU, Y.Q. and FAN, Z. Effects of intensive forced melt convection on the mechanical properties of Fe containing Al-Si based alloys. *Materials Science and Engineering.* 2007. vol. 445-446, pp. 65-72.

[26] SAMUEL, A.M. and SAMUEL, F.H. Effect of alloying elements and dendrite arm spacing on the microstructure and hardness of an Al-Si-Cu-Mg-Fe-Mn (380) aluminum die-casting alloy. *Journal of Materials Science.* 1995, vol. 30, pp. 1698-1708.

[27] GÓRNY, Z. and SOBCZAK, J. *Nowoczesne tworzywa odlewnicze na bazie metali nieżelaznych*. ZA-PIS, Kraków 2005.

[28] PIETROWSKI, S. *Siluminy.* Wydawnictwo Politechniki Łódźkiej, Łódź 2001.

[29] PIETROWSKI, S. *Krystalizacja, struktura i właściwości siluminów tłokowych*, Wydawnictwo, Politechniki Łódźkiej, Łódź 1999.

[30] SHABESTARI, S.G. The effect of iron and manganese on the formation of intermetallic compounds in Al-Si alloys. *Materials Science and Engineering.* 2004. vol. A383, pp. 289-298.

[31] *Fatigue Data Book Light Structural Alloys*. ASM International. The Materials Information Society. Materials Park, OH, USA 1995.

[32] MONDOLFO, L.F. *Manganese in Aluminum Alloys.* The Manganese Center, Paris, 1987.

[33] SHABESTARI, S.G., MAHMUDI, M., EMAMY, M. and CAMPBELL J. Effect of Mn and Sr on intermetallic in Fe-rich eutectic Al-Si alloy. *International Journal of Cast Metals Research.* 2002. vol. 15, iss. 1, pp. 17-24.

[34] BÖSCH, D., PAGATSCHER, ST., HUMMEL, M., FRAGNER, W., UGGOWITZER, P.J., GÖKEN, M. and HÖPPEL, W. Secondary Al-Si-Mg high-pressure die casting alloys with enhanced ductility. *Metallurgical and Materials Transactions.* 2015. vol. 46A, pp. 1035-1045.

[35] TAYLOR J.A. Iron-containing intermetallic phase in Al-Si based casting alloys. *Procedia Materials Science.* 2012. vol. 1, pp. 19-33.

[36] JI, S., YANG, W., GAO, F., WATSON, D. and FAN Z. Effect of iron on the microstructure and mechanical property of Al-Mg-Si-Mn and Al-Mg-Si die cast alloys. *Materials Science and Engineering.* 2013. vol. A564, pp. 130-139.

[37] LUMLEY, R.N., GUNASEGARAM, D.R., GERSHENZON, M. and O'DONELL R.G. Effect of alloying elements on heat treatment response of aluminum high pressure die casting. *International Heat Treatment and Surface Engineering.* 2010. vol.4, no 1, pp. 25-32.